

# Accepted Manuscript

Predicting solubility/miscibility in amorphous dispersions: It's time to move beyond regular solution theories

Bradley D. Anderson



PII: S0022-3549(17)30690-1

DOI: [10.1016/j.xphs.2017.09.030](https://doi.org/10.1016/j.xphs.2017.09.030)

Reference: XPHS 947

To appear in: *Journal of Pharmaceutical Sciences*

Received Date: 15 August 2017

Revised Date: 22 September 2017

Accepted Date: 22 September 2017

Please cite this article as: Anderson BD, Predicting solubility/miscibility in amorphous dispersions: It's time to move beyond regular solution theories, *Journal of Pharmaceutical Sciences* (2017), doi: 10.1016/j.xphs.2017.09.030.

This is a PDF file of an unedited manuscript that has been accepted for publication. As a service to our customers we are providing this early version of the manuscript. The manuscript will undergo copyediting, typesetting, and review of the resulting proof before it is published in its final form. Please note that during the production process errors may be discovered which could affect the content, and all legal disclaimers that apply to the journal pertain.

## Predicting solubility/miscibility in amorphous dispersions: It's time to move beyond regular solution theories

Bradley D. Anderson

Department of Pharmaceutical Sciences

University of Kentucky

Lexington, KY

### ABSTRACT

The evolving challenges associated with the development of poorly soluble drug molecules have been met with major advances in drug solubilization. In particular, amorphous solid dispersion technology is becoming an increasingly important option to enhance oral bioavailability by creating prolonged drug supersaturation to maximize the driving force for intestinal absorption. A primary concern in the development of amorphous solid dispersions is their physical stability, leading to increasing interest in predictive methodologies to assess the propensity for drug crystallization under various storage conditions. For most drug-exipient combinations of pharmaceutical interest, hydrogen-bonding is an important factor in determining miscibility, supersaturation potential, and the influence of water uptake during storage and after administration. The vast majority of publications to date have utilized mathematical models based on regular solution theory such as Flory-Huggins (F-H) theory to predict drug-polymer miscibility, despite the fact that they were never intended to be applied to hydrogen-bonded systems. In this commentary, regular solution theory is applied to simple hydrogen bonded alcohol-alkane solutions to explore trends in the F-H  $\chi$  interaction parameter and possible pitfalls in its interpretation. More recent models that explicitly allow for specific interactions merit greater attention.

Because of the need to develop solution formulations for pharmaceutical agents intended for intravenous administration as well as the recognition that orally administered products must ultimately deliver the drug in solution form in order to achieve good bioavailability, pharmaceutical scientists have always sought better methods to predict, measure, and enhance the equilibrium solubility of new drug candidates. To that end, the contributions of Dr. Samuel Yalkowsky in developing the general solubility equation and its extensions<sup>1</sup> have had a major impact in the field. It is now clear that drug solubilization and solubility prediction have been moving targets over recent decades. As noted by Lipinski two decades ago,<sup>2</sup> the percentage of drug candidates having poor aqueous solubility that have emerged from modern drug discovery efforts has steadily increased in recent years. In 2010, Loftsson and Brewster<sup>3</sup> observed that “while 40% of currently marketed drugs are poorly soluble based on the definition of the biopharmaceutical classification system (BCS), about 90% of drugs in development can be characterized as poorly soluble”. More recently Taylor and Zhang commented that while an equilibrium solubility of 100 µg/mL may have been considered to be highly insoluble in the 1990’s, today’s scientists “feel fortunate” if the aqueous solubility of a drug candidate is 10 µg/mL.<sup>4</sup>

This evolving solubility challenge has been met with an increasing emphasis on the developability of drug candidates in early discovery<sup>5,6</sup> as well as various advanced drug solubilization strategies. Among the latter, formulation approaches that lead to prolonged drug supersaturation to maximize the driving force for sustained intestinal absorption of an oral product<sup>4,7-9</sup> or to allow sufficient time for injection after reconstitution of a parenteral lyophile formulation<sup>10</sup> have attracted increasing interest. Among these, the rise in number of patents and publications relating to amorphous pharmaceuticals and pharmaceutical dispersions (ASDs) over the last three decades has been quite dramatic, as illustrated in Figure 1. ASDs typically consist of an active pharmaceutical ingredient (API) intimately dispersed at a molecular level with an excipient such as an amorphous sugar or polymer to form a glassy solid. After oral administration, dissolution of this amorphous solid can produce supersaturated concentrations of the API that, if prolonged, may provide superior bioavailability compared to products containing crystalline drug.

Numerous recent reviews summarize the process of amorphization, supersaturation potential, and stability/miscibility of ASDs.<sup>4,11-14</sup>

Accompanying the increase in the number of patents and publications related to amorphous pharmaceutical dispersions has been a corresponding relative increase in the application of various solution theories or computational methods to predict the propensity for phase separation of the components in these mixtures.<sup>12,15</sup> While several factors that can be broadly characterized as either kinetic or thermodynamic components are involved in stabilizing amorphous dispersions, it is generally assumed that the maximum physical stability defined in terms of inhibition of drug crystallization requires that the drug and excipient remain intimately mixed. Phase separation of the drug from its excipient may be the first step that ultimately leads to crystallization. Moisture uptake may induce phase separation either by increasing mobility in the ASD through effects on  $T_g$ , altering the solution thermodynamics of the system by increasing the free energy of mixing to the point where phase separation is thermodynamically favored, or both. The focus of this article is on predicting the driving forces for phase separation and eventual drug crystallization as governed by the thermodynamics of these metastable systems. The degree to which amorphous dispersions provide supersaturated solutions of the API also reflects the thermodynamic driving forces governing the drug's escaping tendency during the dissolution process. Though not emphasized herein, the role of kinetic factors and mobility in determining both the shelf-life of ASD products and the extent to which the supersaturation potential can be realized and maintained cannot be overlooked. Readers may want to refer to numerous recent reviews addressing these kinetic factors.<sup>16-19</sup>

#### *Regular Solution Theories to Predict Drug-Excipient Miscibility in ASDs*

The vast majority of publications to date have utilized mathematical models based on regular solution theory to predict drug-polymer miscibility. Regular solutions differ from ideal solutions solely due to the enthalpy of mixing term. In ideal solutions the enthalpy of mixing,  $\Delta H_{mix}$  is always zero, so that the molar Gibbs free energy of mixing is determined entirely by the entropy of mixing,  $\Delta S_{mix}$ :

$$\Delta S_{mix} = -R \sum_i x_i \ln x_i \quad [1]$$

where  $R$  is the universal gas constant and  $x_i$  is the mole fraction of component  $i$  in the solution. The change in the Gibbs free energy,  $\Delta G_{mix}$ , on mixing two components A and B at a given temperature  $T$  is then:

$$\Delta G_{mix} = RT(x_A \ln x_A + x_B \ln x_B) \quad [2]$$

For an ideal solution  $\Delta G_{mix}$  is always negative (favorable) because the ideal entropy of mixing is positive ( $\Delta G_{mix} = \Delta H_{mix} - T \Delta S_{mix}$ ). Thus, the components that form an ideal solution are always completely miscible.

The entropy of mixing can be readily derived from lattice models (for an introduction, see Dill & Bromberg<sup>20</sup>) in which the components are assumed to be identical in size and each molecule is randomly placed into one site in the lattice until the lattice is completely filled. The entropy of mixing is determined by the number of distinguishable arrangements,  $W_{solution}$ , of the A and B molecules on the lattice in the mixture where  $N_A$  and  $N_B$  are the numbers of molecules of each component.

$$\Delta S_{mix} = S_{soln} - S_{pure\ A\&\ B} = k \ln W_{soln} = k \ln \frac{N!}{N_A! N_B!} = k(N \ln N - N_A \ln N_A - N_B \ln N_B) \quad [3]$$

Regular solutions deviate from ideality in that the change in enthalpy on mixing,  $\Delta H_{mix}$ , is not zero. However, the entropy of mixing is assumed to be the same as that for an ideal solution as the interactions between the components are sufficiently weak that the random mixing found in ideal solutions is preserved. Strong interactions, such as hydrogen bonding interactions that lead to the formation of molecular complexes, cause deviations from the random mixing associated with the ideal entropy.

The enthalpy change on mixing two small molecules A and B derived from lattice models of regular solutions is

$$\Delta H_{mix} = RT x_A x_B \chi_{AB} \quad [4]$$

where

$$\chi_{AB} = \frac{z}{kT} \left( w_{AB} - \frac{1}{2} (w_{AA} + w_{BB}) \right) = \frac{z}{kT} \Delta w \quad [5]$$

The quantity  $\chi_{AB}$ , referred to as the exchange or interaction parameter, is a dimensionless quantity that reflects the difference between the AB contact energy and the average of the contact energies for each of the pure components A & B,  $\Delta w (= w_{AB} - \frac{1}{2}(w_{AA} + w_{BB}))$ , where  $z$  represents the number of sides (contacts) for each lattice site. The overall result for the free energy of mixing from the lattice model for regular solutions is therefore:<sup>21</sup>

$$\frac{\Delta G_{mix}}{RT} = x_A \ln x_A + x_B \ln x_B + \chi_{AB} x_A x_B \quad [6]$$

Flory-Huggins (F-H) theory represents an extension of the lattice theory for regular solutions to adjust for the size disparity between molecules in solutions containing one or more polymers. The lattice site in F-H theory typically represents a polymer segment and the probability that a given lattice site is occupied by a polymer segment takes into account the polymer chain connectivity. The change in free energy on mixing a drug and polymer (per mole of lattice sites) in F-H theory is then expressed in terms of the volume fractions of the drug and polymer ( $\phi_{drug}$  and  $\phi_{polymer}$ ) rather than mole fractions.<sup>22,23</sup>

$$\frac{\Delta G_{mix}}{RT} = \frac{\phi_{drug}}{m_{drug}} \ln \phi_{drug} + \frac{\phi_{polymer}}{m_{polymer}} \ln \phi_{polymer} + \chi_{drug-polymer} \phi_{drug} \phi_{polymer} \quad [7]$$

where  $m_{drug}$  and  $m_{polymer}$  are the ratios of the volumes of drug and polymer to that of a lattice site. The first two terms in the equation are the combinatorial or entropic contribution and the last term is the enthalpic contribution.

#### *Solubility Parameter Method for Determining $\chi$*

The utility of regular solution theory in predicting miscibility depends on a reliable determination of the chi value. The solubility parameter approach has been one of the most popular methods for estimating the interaction parameter,  $\chi$ , because it only requires knowledge of the properties of the pure components. The original Hildebrand solubility parameter for a given compound,  $\delta$ , was defined as the square root of the cohesive energy density:<sup>24</sup>

$$\delta = \sqrt{\frac{\Delta E_v}{V_m}} \quad [8]$$

where  $\Delta E_v$  is the energy of vaporization and  $V_m$  is the molar volume of the pure component in its condensed phase. In the development of solubility parameters,  $\Delta w$  in Eq. 5 was approximated by assuming that  $w_{AB}$  is equal to the geometric mean of  $w_{AA}$  and  $w_{BB}$  (i.e.,  $w_{AB} = (w_{AA} \cdot w_{BB})^{1/2}$ ). The result was that the interaction parameter,  $\chi_{AB}$ , could be determined solely from the Hildebrand solubility parameters of the two components in the mixture:

$$\chi_{AB} = \frac{v}{RT} (\delta_A - \delta_B)^2 \quad [9]$$

where  $v$  is the volume of a lattice site and  $\delta_A$  and  $\delta_B$  are the pure component solubility parameters. The application of solubility parameters to pharmaceutical systems was reviewed by Hancock et al.<sup>25</sup> twenty years ago and the approach continues to be popular today, as documented in several recent reviews and research articles.<sup>11,12,26,27</sup>

A key shortcoming of the solubility parameter approach is inherent in the form of Eq. 9. Only positive values of  $\chi_{AB}$  result from the  $(\delta_A - \delta_B)^2$  term and therefore only positive deviations from the ideal free energy of mixing or Raoult's law are possible. In that sense, solubility parameter theory is the mathematical equivalent of the maxim "like dissolves like". It cannot account for negative deviations from Raoult's law that are the result of more favorable interactions between the drug and excipient such as the formation of hydrogen-bonded complexes.<sup>28</sup> Yet, despite the fact that the geometric mean assumption limits the utility of Hildebrand solubility parameters to systems in which relatively weak, nonpolar interactions dominate has been recognized for decades,<sup>24</sup> solubility parameter theory remains quite popular.

Recent publications in which the predictions of miscibility in ASDs using solubility parameter theory have been compared to other methods confirm its shortcomings. For example, Marsac et al.<sup>29,30</sup> determined that both felodipine and nifedipine were miscible with PVP at all concentrations, contrary to predictions of solubility parameter theory. ASDs investigated in this author's laboratory using molecular

dynamics simulations have consistently found that estimates of  $\chi$  from solubility parameters fail to predict the free energies of mixing generated from F-H theory without the geometric mean assumption.<sup>31,32</sup>

Hansen solubility parameters represented an attempt to extend solubility parameter theory to include polar and hydrogen bonding interactions.<sup>33,34</sup> Experimental miscibility data were represented in three-dimensional space with axes corresponding to partial solubility parameters describing dispersion ( $\delta_d$ ), polar ( $\delta_p$ ), and hydrogen bonding ( $\delta_h$ ) interactions. However, as pointed out by DeBoyace and Wilfong,<sup>12</sup> Hansen solubility parameters are only semi-empirical as there is “no thermodynamic justification for the separation” of the total solubility parameter into these three components. In particular, they noted that the hydrogen bonding component ( $\delta_h$ ) would not capture the requirement for different functional groups (i.e., a hydrogen bond donor and acceptor) to form a hydrogen bond between the API and excipient. Recognition of this problem led to further splitting of  $\delta_h$  into acidic and basic components.<sup>35</sup> Thakral and Thakral recently applied Hansen solubility parameters to screen 83 drugs for miscibility with polyethylene glycol, suggesting that this approach might be useful for rapidly excluding certain drug-excipient combinations.<sup>36</sup> The empirical nature of this approach, the proliferation of descriptors introduced in an attempt to overcome the limitations of the original solubility parameter theory, and the need for correspondingly large experimental data sets to obtain these parameter estimates limits the predictive value of this approach.

#### *Assumptions in Lattice Theories for Regular Solutions*

The lattice theory for regular solutions (Eq. 6) and F-H theory as described in Eq. 7 do not constrain the value of  $\chi_{AB}$  to positive values as imposed by the geometric mean assumption in solubility parameter theory, and thus it would appear to be suitable for application in a much wider array of pharmaceutical systems, including those having negative  $\chi_{AB}$  values that favor miscibility. However, there are other assumptions in the development of Eqs. 6 and 7 that merit further consideration.<sup>20</sup> One already mentioned is the assumption of ideal entropy. A second important assumption related to the first is the mean-field approximation or the Bragg-Williams approximation. This approximation leads to the mathematical form of the interaction parameter  $\chi_{AB}$  by assuming that the probability that a B molecule occupies a given specific site next to an A molecule is determined solely by the fraction of all sites



occupied by B molecules (i.e., random mixing). Strong interactions such as hydrogen bonding violate both the ideal entropy assumption and the mean-field approximation. Another implicit assumption in the use of Eqs. 6 or 7 is that there is a single  $\chi_{AB}$  value applicable at all solution compositions. The attractiveness of this feature is that determination of a single  $\chi_{AB}$  value allows the prediction of API-excipient miscibilities over the entire composition range.

The above assumptions also factor into the reliability of the interaction parameter values obtained from experimental data that may depend on the method employed. The challenges of generating reliable values of the interaction parameter from experimental data have been the subject of numerous original publications and reviews.<sup>11,12,29</sup> The difficulty stems in part from the lack of equilibrium in glassy matrices which precludes direct solubility measurements. Thus, methods such as melting point depression are employed to probe API-excipient miscibility under pseudo-equilibrium conditions<sup>26,37-39</sup> or API solubilities are measured at room temperature in liquid solvents chemically similar to the polymer of interest (e.g., 1-ethyl-2-pyrrolidone as a chemical equivalent to polyvinylpyrrolidone (PVP)) to obtain estimates of  $\chi$ .<sup>38-41</sup> Both approaches assume the ideal entropy of mixing term in the F-H equation in order to estimate the enthalpic contribution to the free energy derived from solubility measurements. Determining solubility in low molecular weight polymer analogues at room temperature offers the advantage of providing an estimate of  $\chi_{AB}$  that requires no temperature correction while the melting point depression method gives a value of  $\chi_{AB}$  at the melting temperature rather than at room temperature. Also, questions relating to whether or not equilibrium has been achieved in the melting point depression method remain a subject of debate.

Although the likely dependence of  $\chi_{AB}$  on temperature is not explicitly included in the fundamental equations stemming from lattice theory, the relationship between  $\chi_{AB}$  and  $\Delta H_{mix}$  (Eq. 4) and the likely temperature dependence of  $\Delta H_{mix}$  as determined by a probable change in heat capacity on mixing,  $\Delta C_{p,mix}$ , suggests how  $\chi_{AB}$  may depend on temperature. For example, the temperature dependence of the melting enthalpy,  $\Delta H_f$ , measured at the melting point of a pure crystalline API combined with the assumption that  $\Delta C_p$  itself is independent of temperature, has been used to estimate the (ideal) solubility of an amorphous API relative to its crystalline counterpart, at any temperature.<sup>4,42</sup> A similar relationship

has recently been employed to describe the solubility of crystalline API,  $x_{API}$ , in a non-ideal amorphous API/polymer liquid mixture.<sup>43,44</sup>

$$x_{API} = \frac{1}{\gamma_{API}} \exp \left\{ -\frac{\Delta H_{API}^{s \rightarrow l}}{RT} \left( \frac{T_m - T}{T_m} \right) - \frac{\Delta C_{p, API}^{s \rightarrow l}}{R} \left[ \ln \left( \frac{T_m}{T} \right) - \frac{T_m}{T} + 1 \right] \right\} \quad [10]$$

where  $\Delta H_{API}^{s \rightarrow l}$  and  $\Delta C_{p, API}^{s \rightarrow l}$  are the changes in enthalpy and heat capacity for the transfer of API from the solid phase to the API/polymer liquid phase at the melting temperature,  $T_m$ , respectively.  $\Delta C_{p, API}^{s \rightarrow l}$  for pharmaceutical materials is typically non-zero.  $\gamma_{API}$  accounts for the activity coefficient of the API in the API/polymer liquid phase. Noting that  $\Delta C_{p, API}^{s \rightarrow l}$  is usually neglected in the application of F-H models, Lehmkemper et al.<sup>43</sup> argued that it should be included to improve the accuracy of solubility calculations.

Note that if  $\Delta C_p$  for a given process is not zero, then both  $\Delta H$  ( $= \int_{T_1}^{T_2} \Delta C_p dT$ ) and  $\Delta S$  ( $= \int_{T_1}^T \frac{\Delta C_p}{T} dT$ ) depend on temperature.

Lin and Huang<sup>45</sup> adopted a less complex linear relationship between the F-H interaction parameter,  $\chi$ , and  $1/T$  than suggested by the above equation to predict the solubility of API in a polymer excipient at any temperature from the melting points of binary ASDs at varying composition as described in Eq. 11. A previously reported empirical linear relationship between  $\chi$  and  $1/T$  was assumed<sup>23</sup> from which two constants A and B could be determined by fitting the values of  $\chi$  at varying composition to Eq. 11. The constant A is assumed to reflect a noncombinatorial entropic contribution while B relates to the enthalpic contribution. The constants are considered invariant with temperature and composition.

$$\chi = A + \frac{B}{T} \quad [11]$$

Values of  $\chi$  used in Eq. 11 were estimated from melting point depression data for mixtures at varying composition (i.e.,  $1/T_m - 1/T_m^0 = -R/\Delta H_f (\ln \phi + (1-1/m)(1-\phi) + \chi(1-\phi)^2)$ , where  $T_m^0$  is the melting point of the pure crystalline drug,  $T_m$  (i.e., the value of T in Eq. 11) is the melting point in a drug/polymer mixture at a drug volume fraction of  $\phi$ , m is the ratio of the volume of a polymer chain to that of the drug molecule, R is the gas constant, and  $\Delta H_f$ , the heat of fusion of the pure drug, which was assumed to be constant).

The above experimental methods are indirect in the sense that  $\chi$  is estimated from melting point depression after correcting for the ideal entropy of mixing combined with an empirical (non-ideal) entropy correction constant (A in Eq. 11). Accounting for the temperature dependence of  $\chi_{AB}$  through an empirical relationship diminishes to some extent the attractiveness of regular solution theories such as F-H theory to generate complete drug-excipient phase diagrams because now two parameters must be obtained from the experimental data, requiring expanded data sets. Moreover, Tian et al.<sup>27</sup> employed Eq. 11 and melting point depression data to construct phase diagrams for felodipine in three polymeric excipients (polyvinylpyrrolidone (PVP) K-15, polyvinyl caprolactam-polyvinyl acetate-polyethylene glycol (Soluplus), and hydroxypropyl methyl-cellulose acetate succinate (HPMCAS)). Significant deviation was observed with elevated temperatures, suggesting that the actual temperature dependence of  $\chi_{AB}$  does not conform to Eq. 11 (see also Knopp et al.<sup>46</sup>).

DeBoyace and Wildfong<sup>12</sup> observed that, to date, phase diagrams for only a few APIs in amorphous dispersions (i.e., aceclofenac, felodipine, indomethacin, and ketoconazole) have been published. This may stem from the necessity to conduct more experiments to generate the temperature dependence of  $\chi_{AB}$  as well as concerns regarding the accuracy of the linear transformation. However, there are other concerns.

Several researchers including Lin and Huang, have noted that the use of Eq. 11 requires the possible dependence of  $\chi_{AB}$  on drug concentration to be neglected. Manias & Utracki<sup>47</sup> observed that in polymer solutions  $\chi_{AB}$  has a complex dependence on many independent variables, with nine parameters necessary to describe the variation of  $\chi_{AB}$  with concentration and temperature at constant pressure. In a recent study of drug-polymer miscibility in ASDs, Baghel et al.<sup>48</sup> employed Eq. 11 but, citing Koningsveld et al.,<sup>49</sup> they cautioned that  $\chi_{AB}$  displays a “non-trivial dependence on the temperature and volume fraction of the polymer”. In using a ternary F-H model to generate  $\chi_{\text{drug-polymer}}$  values for cinnarizine in PVP and polyacrylic acid (PAA) from moisture sorption data, they were able to demonstrate a significant dependence of  $\chi_{\text{drug-polymer}}$  on the weight fraction of drug from 10-65%, with interaction parameter values ranging from approximately  $-3$  for ASDs containing 10% API in PVP to nearly zero at 65% weight fractions of API in either PVP or PAA.

### *ASDs are Typically Hydrogen-Bonded Systems*

Most of the ASD formulations that have been explored are hydrogen bonding systems. In a recent review, Baghel et al.<sup>11</sup> provided a table containing examples of different polymers and drugs that had been explored in various types of amorphous dispersion. Of the APIs in this compilation having known structures, 84% possessed hydrogen bond donor and acceptor functional groups while the remaining compounds had multiple hydrogen acceptor groups. Most of the studies in which the API had only hydrogen acceptor functional groups were with excipients that possessed hydrogen bond donors. Thus, nearly all examples are hydrogen bonded systems that likely violate key assumptions that form the basis for regular solution theories.

In our laboratory, molecular dynamics (MD) simulations have been conducted for a number of amorphous drugs,<sup>50</sup> polymers,<sup>32,51-53</sup> and drug-excipient solid dispersions<sup>31,32</sup> to explore the utility of such simulations for characterizing the intermolecular interactions and their effects on miscibility. In every case, hydrogen bonding interactions have been important. For example, one model ASD, indomethacin(IND)-PVP, has been explored extensively both experimentally and by MD simulations to probe the intermolecular interactions, drug-excipient miscibility, API solubility enhancement, and other properties.<sup>31,54-67</sup>

Indomethacin contains both hydrogen donor and acceptor functional groups (i.e., -COOH, -CONH-, and -OCH<sub>3</sub>) that can participate in hydrogen bonding interactions. In MD simulations of pure amorphous IND, 79% of the molecules were found to participate in at least one hydrogen bonding interaction leading to the formation of cyclic aggregates such as dimers and linear chains.<sup>50</sup> Solid-state NMR experiments were in excellent agreement with these results. In IND-PVP dispersions, disruption of IND self-association occurs due to dilution in the excipient and competing hydrogen bond formation between the IND-COOH and PVP >C=O groups to form drug-polymer complexes, as demonstrated in MD simulations as well as SSNMR, infrared, and x-ray studies.<sup>58,64,67</sup> The extent to which this occurs depends on the relative concentrations of IND and PVP in the ASD. The result is a favorable enthalpy of mixing and good miscibility for IND-PVP amorphous dispersions. Qualitatively similar patterns have been observed in MD simulations of felodipine (FEL)-hydroxypropyl methylcellulose (HPMC) amorphous

dispersions, even though the >NH group in felodipine is a much weaker hydrogen donor than the –COOH group in indomethacin.<sup>32</sup> In amorphous FEL, approximately 40% of the FEL >NH groups were found to be involved in hydrogen bonds with other felodipine molecules by MD simulation. These were replaced to some extent in a FEL-HPMC ASD (62%/38% wt/wt) containing only a trace of water while at a higher water content (10.5%), most FEL-FEL hydrogen bonds were disrupted to form hydrogen bonds with water.

Water uptake in ASDs leads to systems that most certainly deviate from the assumptions of regular solution theory. Molecular dynamics simulations of ASDs containing water conducted in our laboratory and others consistently indicate a strong tendency for water to form hydrogen bonded clusters even at relatively low water concentrations.<sup>31,32,50,52,53</sup> For example, in PVP at 0.5% water, individual water molecules were found to exist mostly as monomers hydrogen bonded to PVP with only a small fraction of water dimers. At 10% water, most water molecules were present in water clusters with each water molecule involved in hydrogen bonds to two adjacent water molecules plus an oxygen atom of a PVP >C=O.

Given the predominance of H-bonding APIs and excipients in ASDs that have been analyzed using regular solution lattice models such as the F-H theory along with the critical importance of water uptake, it might be instructive to test F-H theory in simpler equilibrium systems in which hydrogen bonding is known to play an important role. This author's introduction to pharmaceutical research many years ago involved studies of the self-association of alcohols in hydrocarbon solvents using solution calorimetry<sup>68</sup> and vapor-liquid equilibria.<sup>69,70</sup> The vapor-equilibria studies involved determination of relative alcohol vapor pressures by sampling the head space above solutions of various alcohols in isooctane and analyzing the vapor concentration of alcohol by gas chromatography. One alcohol in particular, octanol, has been particularly important in the pharmaceutical sciences as exemplified by the widespread adoption of the Hansch  $\pi$  values based on octanol/water partition coefficients as a measure of lipophilicity in the development of quantitative structure activity relationships.<sup>71</sup> Apparently, octanol mimics the solvent properties of diverse types of biological lipids although why this is the case is not yet fully understood. The general solubility equation and its extensions developed by Yalkowsky and his colleagues,<sup>1,72,73</sup> among the most widely applied equations for predicting the water or cosolvent solubility

of an API, are based on knowledge of the compound's melting point and lipophilicity, as measured by the octanol/water partition coefficient. In these equations, the transfer of API from its supercooled melt to water is approximated by the octanol/water partition coefficient. Thus, octanol is assumed to mimic the solvent properties of the supercooled melt of the API, regardless of the API's structure!

#### *Application of Regular Solution Theory to Well-Known Hydrogen-Bonded Solutions*

Our early work and that of others demonstrated that in hydrocarbon solvents, alcohols tend to self-associate to form cyclic n-mers. On average, primary alcohols varying in chain length from C3-C8 were found to preferentially form cyclic pentamers with increasing concentration in isooctane.<sup>70</sup> Moreover, plots of monomer concentration versus the total molar concentration of alcohol were superimposable up to one molar for all chain lengths, indicating that it is the –OH molar concentration that governs the thermodynamic activity of the alcohol. Pure octanol was found to consist largely of aggregates with less than 5% present as monomer. More recent experimental studies as well as MD simulations have generally confirmed these conclusions while adding more detail. MD simulations of pure octanol and hydrated octanol by MacCallum and Tieleman<sup>74</sup> suggested that a variety of structures co-exist in pure octanol with a large fraction of the octanol present in clusters of 4-7 molecules. The fraction of “free” hydroxyl groups (i.e., monomer) in pure octanol was 5.5% in the MD simulations, matching our earlier experimental results. Fouad et al.<sup>75</sup> recently combined their MD simulations with experimental data for the free monomer fraction in various binary systems of alcohol + alkane to demonstrate that the monomer fractions overlap when plotted against the molar concentration of association sites (rather than mole fraction or volume fraction).

Shown in Fig. 2 are plots generated from a report by Gracia et al.<sup>76</sup> on the vapor pressures above solutions of 1-butanol and n-hexane at various mole fractions of butanol and at several temperatures between 283.1 K and 323.12 K. The data in Fig. 2 are at 283.1 K, 298.11 K, and 323.12 K, corresponding to 10 °C, 25 °C, and 50 °C. The lower curve reflects the calculated ideal free energy of mixing divided by RT,  $\Delta G_{\text{ideal}}/RT$ , assuming an ideal entropy contribution from random mixing and zero enthalpy of mixing. The middle curve is the observed free energy of mixing over RT,  $\Delta G_{\text{mix}}/RT$ , from the experimental vapor pressure data of Gracia et al., and the upper curve represents the excess free energy of mixing over RT,  $\Delta G_{\text{excess}}/RT$ , obtained from the difference between the experimental and ideal free

energies at each solution composition and temperature. It is clear from the positive values of the excess free energy curve that mixing butanol and hexane is much less favorable than that predicted for an ideal solution, yet these compounds remain miscible at all compositions over the temperature range explored, as evident in the observed  $\Delta G_{\text{mix}}/RT$  profile. The positive excess free energy suggests that the enthalpy of mixing butanol with alkane solvents is positive. Indeed, the enthalpy of mixing is quite positive (unfavorable) as demonstrated in our previous calorimetric studies where the enthalpy required for dissociation of a cyclic aggregate was found to be  $\sim 5$  kcal/mol/bond.<sup>68</sup> However, the excess free energy is only modestly positive, suggesting that the unfavorable enthalpy of mixing is largely compensated for by a favorable entropy of mixing when aggregates dissociate, a component that is not taken into account in classical F-H theory. Values of the F-H interaction parameter,  $\chi_{AB}$ , were obtained as a function of butanol concentration from  $\Delta G_{\text{mix}}/RT$  (middle curve) by applying either Eq. 6 or Eq. 7. Given the similarity in molecular size of butanol and hexane, the results are virtually the same using either mole fractions (Eq. 6) or volume fractions (Eq. 7) of butanol.

The values of  $\chi_{AB}$  obtained from the data at the three temperatures in Fig. 2 are plotted in Fig. 3 versus the mole fraction of butanol. Three observations are noteworthy. First, the apparent  $\chi_{AB}$  values are negative, suggesting a negative value for the heat of mixing according to Eq. 4, in contrast to the positive values obtained calorimetrically. Second, contrary to expectations from the classical F-H theory equation, no single  $\chi_{AB}$  value can account for the free energy of mixing over the entire composition range, with values becoming significantly more negative at both the low and high mole fractions of alcohol. Third, the apparent temperature dependence of  $\chi_{AB}$  is rather small except in the range of high alcohol dilution (where self-association is becoming completely disrupted).

More insight can be gained by examining vapor-liquid equilibria data generated by Van Ness et al.<sup>77</sup> for the thermodynamics of mixing ethanol and heptane. They combined heats of mixing from isothermal calorimetry over a temperature range of 10 °C to 75 °C with vapor pressures to obtain enthalpies, heat capacities, entropies, and free energies of mixing as well as the excess free energies and entropies. Shown in Fig. 4 are values for  $\Delta H_{\text{mix}}/RT$  (upper curves),  $\Delta G_{\text{mix}}/RT$  (middle curves), and  $-\Delta S_{\text{mix}}/R$  (lower curves) versus the mole fraction of ethanol at 5 °C, 25 °C, and 40 °C. As observed previously in Fig. 2 for butanol in hexane,  $\Delta G_{\text{mix}}/RT$  is slightly negative indicating that ethanol and

heptane are completely miscible at these temperatures. Van Ness et al. reported a heat of dilution (to infinite dilution) for ethanol of 23,600 J/mol equivalent to 5.6 kcal/mol, similar to the value of 5 kcal/mol for dissociation of hydrogen bonds in butanol – alkane mixtures.<sup>68</sup> The heat of mixing data ( $\Delta H_{\text{mix}}/RT$ ) in Fig. 4 provide significant new information not available in Fig. 2. First,  $\Delta H_{\text{mix}}/RT$  is quite dependent on temperature indicating a positive  $\Delta C_{p_{\text{mix}}}$ . More importantly, a substantial enthalpy-entropy compensation is evident in Fig. 4. Decreases in the positive enthalpy of mixing at lower temperature are counterbalanced by less favorable excess entropies of mixing and vice versa for increasing temperatures, leading to nearly superimposable profiles for the free energies of mixing,  $\Delta G_{\text{mix}}/RT$ , over this temperature range.

The F-H interaction parameter,  $\chi_{AB}$ , could be obtained in two ways from the data in Fig. 4 – directly from the heats of mixing (Eq. 4) which involves no assumption regarding the entropy term, or from the  $\Delta G_{\text{mix}}/RT$  profiles according to Eq. 6 or Eq. 7, where  $\chi_{AB}$  is normally obtained from  $\Delta G_{\text{mix}}/RT$  after subtracting the ideal entropy of mixing. The results obtained using these two methods are shown in Fig. 5. Not surprisingly,  $\chi_{AB}$  values determined directly (i.e., calorimetrically) from  $\Delta H_{\text{mix}}/RT$  are uniformly positive. This is the expected result given Eq. 4 and the positive enthalpies of mixing for alcohols in hydrocarbons. These  $\chi_{AB}$  values are relatively constant above 0.1 mole fraction of ethanol, becoming quite large in more dilute solutions reflecting the concentration region where substantial dissociation of ethanol aggregates occurs. In contrast, the  $\chi_{AB}$  values obtained from  $\Delta G_{\text{mix}}/RT$  profiles are slightly negative, becoming more negative at the low and high ends of the ethanol concentration range. Clearly  $\chi_{AB}$  estimates from these  $\Delta G_{\text{mix}}/RT$  profiles are incorrect because the enthalpy of mixing is positive. This is because the method improperly assumes ideal entropies of mixing. The more accurate values of  $\chi_{AB}$  obtained from  $\Delta H_{\text{mix}}/RT$  also deviate from the F-H theory in that there is a marked composition dependence (recall that the mean-field approximation that provides the simple mathematical form for  $\chi_{AB}$  does not apply for hydrogen bonded systems). Unfortunately, the use of  $\chi_{AB}$  values obtained from enthalpies of mixing to generate free energies and miscibility information from F-H theory and assuming ideal entropies of mixing may also be problematic because the entropy term deviates significantly from ideality. Molecular dynamics simulations also generate  $\chi_{AB}$  directly from Helmholtz interaction energies



(PV work is assumed to be negligible) and thereby also require an estimate of the entropy in order to convert  $\chi_{AB}$  values to free energies. Entropies may be determined if reliable estimates of heat capacities can be generated, but this demands highly precise enthalpy measurements.

While nearly all ASDs explored thus far are hydrogen bonded systems to one degree or another, the alcohol-hydrocarbon systems represent a simplified case study in that only one of the two components can form hydrogen bonds. Generally, both API and excipient (and water, if present) can participate in hydrogen bonding. Such systems are more complex than the examples explored above. Nevertheless, the time has come for pharmaceutical scientists to move beyond models based on regular solution theory to explore models that take specific interactions into account.

#### *A Sampling of Models That Include Specific Interactions such as Hydrogen-Bonding*

Many refinements and extensions of the classical F-H lattice theory have been proposed over the years to address shortcomings in the original equation (Eq. 7) typically employed in modeling ASDs of pharmaceutical interest considered herein. Flory addressed self-association of solution components within the context of a lattice model by including additional n-mers each characterized by the same free energy change on dilution to a monomer standard state.<sup>78</sup> Kretschmer and Wiebe<sup>79</sup> applied the F-H expression for free energy to alcohol-hydrocarbon mixtures by assuming an equilibrium constant, K, for hydrogen-bond formation in terms of molarity rather than mole fraction concentrations. The same value for the equilibrium constant for formation of an additional H-bond was assumed regardless of n-mer size. Experimental data for ethanol and methanol self-association in hydrocarbon solvents were fit to obtain values for K and the F-H exchange parameter. Both the energy of mixing and entropy of mixing terms were dependent on K. For a more comprehensive review of various association models see the book by Acree.<sup>80</sup>

One particularly relevant extension of Eq. 7 is that of Coleman-Painter<sup>81-84</sup> who incorporated an additional term,  $\Delta G_H$ , to account for the effects of specific interactions in polymer blends. The resulting free energy of mixing equation is shown below:

$$\frac{\Delta G_{mix}}{RT} = \left[ \frac{\phi_A}{m_A} \ln \phi_A + \frac{\phi_B}{m_B} \ln \phi_B + \chi_{AB} \phi_A \phi_B \right] + \frac{\Delta G_H}{RT} \quad [12]$$

where the first term in brackets is Eq. 7 and the subsequent terms reflect the excess free energy of mixing attributable to A-B and B-B hydrogen bond formation, having the respective association constants  $K_{AB}$  and  $K_B$ . For mixing a polymer B that self-associates through hydrogen bonding with a polymer A that does not self-associate but forms A-B hydrogen-bonded complexes, the following form for  $\Delta G_H/RT$  was obtained:

$$\frac{\Delta G_H}{RT} = \phi_B \ln \left[ \frac{\phi_{B1}}{\phi_{B1}^0 \phi_B^{1/n_H^0}} \right] + \frac{\phi_A}{r} \ln \left[ \frac{\phi_{0A}}{\phi_A} \right] + K \phi_B [\phi_{B1} - \phi_{B1}^0] + \phi_B [1 - K \phi_{B1}] \left[ \frac{x}{1-x} \right] \quad [13]$$

where  $\phi_A$  and  $\phi_B$  are the volume fractions of polymers A and B,  $\phi_{0A}$  is the volume fraction of unassociated polymer A,  $\phi_{B1}$  and  $\phi_{B1}^0$  are the volume fractions of non-bonded B monomers in the blend and neat state, respectively,  $n_H^0$  is the number average length of the hydrogen-bonded B chain,  $r = V_A/V_B$  is the ratio of molar volumes, and  $K$  is the association constant for formation of a new B-B hydrogen bond, regardless of chain length. The quantity  $x (=K_{AB}\phi_{0A}/r)$  represents the equilibrium constant for formation of an A-B hydrogen bond with any B-mer. The original theory has since been further refined.<sup>85</sup> and extended to two self-associating fluids<sup>86,87</sup> and excipient-water interactions.<sup>88</sup> The equilibrium constants have been determined experimentally using various spectroscopic methods, most frequently by infrared spectroscopy.<sup>89-91</sup> The temperature dependence of the equilibrium constants must also be determined in order to construct phase diagrams at constant pressure.<sup>92</sup> The utility of the approach is often limited by the difficulties encountered in experimentally determining the needed equilibrium constants.

Off-lattice models in which molecules are distributed throughout continuous three-dimensional space are also gaining attention. One promising example that has attracted recent interest for predicting miscibility in pharmaceutical amorphous dispersions is the perturbed chain statistical association theory (PC-SAFT) equation of state model developed by Gross and Sadowski.<sup>93,94</sup> Equations of state for predicting vapor-liquid phase equilibria based on statistical mechanical methods such as perturbation theory have a long history of development. The reader is referred to the brief history and key references cited by Gross and Sadowski for background information. As described in recent publications wherein PC-SAFT has been applied to API/polymer amorphous dispersions, each molecule within PC-SAFT is reduced to a chain of spherical segments, each of which may interact with other segments of other

molecules via hard-chain repulsions, van der Waals attractions, dipole-dipole interactions, and hydrogen bonding at specific association sites.<sup>95</sup> For example, Prudic et al represented the molecule indomethacin in PC-SAFT<sup>95</sup> as a chain of five spherical segments with six association sites,  $N_i^{\text{association}}$ , to approximate the locations of various sites in the molecule that may participate in specific hydrogen bonding interactions (Fig. 6).

The residual Helmholtz energy,  $a^{\text{res}}$ , can be calculated in PC-SAFT as the sum of various contributions<sup>95</sup> that may include, for a neutral molecule, a hard-chain contribution ( $a^{\text{hc}}$ ), a dispersion term for the van der Waals interactions ( $a^{\text{disp}}$ ), a polar contribution ( $a^{\text{polar}}$ ), and an association (i.e., H-bonding) contribution ( $a^{\text{assoc}}$ ) for each spherical segment. Each of the above contributions represent summations over all segments. For a pure non-polar molecule,  $a^{\text{res}}$  could be represented by  $a^{\text{hc}} + a^{\text{disp}}$ , where  $a^{\text{hc}}$  depends on the number of segments ( $m_i$ ) and the segment diameter,  $\sigma_i$ , and  $a^{\text{disp}}$  is described in terms of a dispersion energy parameter  $u/k$ , where  $k$  is the Boltzmann constant. Thus, 3 parameters are needed to describe each pure nonpolar component. The contribution of association,  $a^{\text{assoc}}$ , to the Helmholtz residual energy for a pure component reflects a summation over all segments and all association sites,  $N_i^{\text{association}}$ ,<sup>96</sup> in terms of two more parameters, an association energy parameter ( $\epsilon^{\text{AiBi}}/k$ ) and an effective association volume related to the distance necessary to form a hydrogen bond,  $\kappa^{\text{AiBi}}$ . Therefore, five parameters would be used to characterize a pure compound that interacts only through dispersion forces and hydrogen bonding. In predicting the phase behavior of several APIs, including indomethacin, in different polyethylene glycols, Prudic et al.<sup>95</sup> assumed that  $a^{\text{res}} = a^{\text{hc}} + a^{\text{disp}} + a^{\text{assoc}}$  (i.e.,  $a^{\text{polar}}$  was not included). Entire phase diagrams generated using PC-SAFT were judged to be in good accordance with the experimental data. While the authors did not compare their results to treatments using F-H theory, they noted that the parameters generated for pure components have a physical meaning and, once determined, can be used to predict the phase diagram for any combination of those components at any concentration, temperature, or pressure.

Later studies by some of the same authors have explored the phase behavior of indomethacin/poly(lactic-co-glycolic acid) (PLGA) formulations as a function of the copolymer composition and molecular weight successfully modelled using PC-SAFT<sup>97</sup> and solid dispersions of indomethacin and

naproxen in polyvinylpyrrolidone (PVP), polyvinyl acetate (VAc), and polyvinylpyrrolidone/vinyl acetate (PVP/VA) copolymers.<sup>98</sup> The effect of absorbed water on the API solubility in the same polymers (PVP, VAc, and PVP/VA) was successfully predicted using PC-SAFT and the Gordon-Taylor equation, respectively.<sup>99</sup>

Luebbert et al.<sup>44</sup> used PC-SAFT to model the solubilities of crystalline ibuprofen and felodipine in PLGA formulations by fitting a single binary interaction parameter to solubility data measured by DSC. They then correctly predicted amorphous phase separation in ibuprofen/PLGA formulations and the absence of amorphous phase separation in felodipine/PLGA formulations. The ibuprofen/PLGA phase separation was more likely at higher drug loading. The predicted influence of the glycolic acid composition in the polymer on amorphous phase separation was in almost quantitative agreement with the experimental results.

Lehmkemper et al.<sup>43</sup> compared the predicted solubilities of acetaminophen and naproxen in PVP K25 and PVP/VA64 using three models: PC-SAFT, F-H theory, and an empirical model developed by one of the authors.<sup>100</sup> They then evaluated the abilities of these models to predict the influence of relative humidity (RH) on API solubility and long-term stability. All of the models were satisfactory in fitting the experimental solubility data which were only accessible by DSC at high temperatures but there were substantial differences in the model predictions at room temperature. Generally, the F-H model predicted a lower solubility at room temperature than PC-SAFT. The difference was attributed to the fact that PC-SAFT accounts for the temperature-dependence of hydrogen bond formation, resulting in higher predicted API solubilities using PC-SAFT. Stability studies at 60% or 75% RH and at temperatures in which supersaturated acetaminophen ASDs were not kinetically stabilized (i.e., above  $T_g$ ) led to the conclusion that F-H theory underestimated the solubility of acetaminophen in both polymers while PC-SAFT reliably distinguished between stable amorphous systems and unstable systems prone to recrystallization. For naproxen ASDs, both F-H and PC-SAFT correctly predicted recrystallization in all samples during the stability study.

Finally, returning to alcohol self-association, Fouad et al.<sup>75</sup> recently demonstrated that the association term in PC-SAFT was necessary to account for the composition dependence of the activity

coefficients of short-chain primary alcohols (methanol through 1-butanol) in several alkane solvents in comparison to models that do not consider self-association (e.g., UNIQUAC). However, this work also provides insight into other aspects of PC-SAFT that may need refinement depending on the system under investigation. In the same study they also found that modifying PC-SAFT to include an additional term for long-range polar interactions (i.e.,  $a^{\text{polar}}$ ) significantly improved the predictions for the fractions of free monomer obtained experimentally from vapor-liquid equilibria and their temperature dependence. Also, selecting the correct number of association sites was found to be important, as a three-site association model for methanol was superior while a two-site model sufficed for the longer chain alcohols. Even with these refinements, Polar PC-SAFT significantly overpredicted the fraction of dimers in the self-associated alcohol-alkane systems in comparison to molecular dynamics simulations. This was taken as new evidence for the importance of modeling the cooperativity of hydrogen bonding to account for the polarization that results from H-bond formation, leading to an increased tendency to form further hydrogen bonds. Overall, this study illustrates that further refinements are likely as more systems are explored using PC-SAFT.

#### *Concluding Remarks*

In conclusion, for decades F-H theory has provided a foundation for predicting the thermodynamic stability of amorphous dispersions despite the fact that the theory was never intended for systems in which hydrogen bonding interactions are important, as is the case for most ASDs. Given the critical importance of the  $\chi$  value, the single parameter in F-H theory necessary to predict miscibility or lack thereof, much emphasis has been placed on the most appropriate methods for obtaining a correct value for this parameter. Less attention has been paid to whether or not the underlying framework is adequate for these complex mixtures. Fortunately, new solution models based on more realistic assumptions are being explored by some pharmaceutical scientists. It is time to move beyond F-H theory, considering the limitations imposed by its assumptions.

## REFERENCES

1. Yalkowski SH. 1999. Solubility and Solubilization in Aqueous Media. New York: Oxford University Press.
2. Lipinski CA, Lombardo F, Dominy BW, Feeney PJ 1997. Experimental and computational approaches to estimate solubility and permeability in drug discovery and development settings. *Adv Drug Deliv Rev* 23:3-25.
3. Loftsson T, Brewster ME 2010. Pharmaceutical applications of cyclodextrins: basic science and product development. *J Pharm Pharmacol* 62:1607-1621.
4. Taylor LS, Zhang GGZ 2016. Physical chemistry of supersaturated solutions and implications for oral absorption. *Adv Drug Deliv Rev* 101:122-142.
5. Butler JM, Dressman JB 2010. The developability classification system: Application of biopharmaceutics concepts to formulation development. *J Pharm Sci* 99:4940-4954.
6. Meanwell NA 2015. The influence of bioisosteres in drug design: Tactical applications to address developability problems. *Top Med Chem* 9:283-381.
7. Leuner C, Dressman J 2000. Improving drug solubility for oral delivery using solid dispersions. *Eur J Pharm Biopharm* 50(1):47-60.
8. Porter CJH, Pouton CW, Cuine JF, Charman WN 2008. Enhancing intestinal drug solubilization using lipid-based delivery systems. *Adv Drug Deliv Rev* 6:673-691.
9. Yeap YY, Trevaskis NL, Porter CJH 2013. The potential for drug supersaturation during intestinal processing of lipid-based formulations may be enhanced for basic drugs *Mol Pharmaceutics* 10:2601-2615.
10. Xiang T-X, Anderson BD 2002. Stable supersaturated aqueous solutions of siltacetan 7-t-butyl-dimethylsilyl-10-hydroxycamptothecin via chemical conversion in the presence of a chemically modified  $\beta$ -cyclodextrin. *Pharm Res* 19:1215-1222.
11. Baghel S, Cathcart H, O'Reilly NJ 2016. Polymeric amorphous solid dispersion: A review of amorphization, crystallization, stabilization, solid-state characterization, and aqueous solubilization of biopharmaceutical classification system class II drugs. *J Pharm Sci* 105:2527-2544.
12. DeBoyace K, Wildfong PLD 2017. The application of modeling and prediction to the formation and stability of amorphous solid dispersions. *J Pharm Sci*.
13. Newman A editor 2015. *Pharmaceutical Amorphous Solid Dispersions*. ed., Hoboken, N.J.: John Wiley & Sons, Inc.
14. Edueng K, Mahlin D, Bergstrom CAS 2017. The need for restructuring the disordered science of amorphous drug formulations. *Pharm Res* 34:1754-1772.
15. Meng F, Dave V, Chauhan H 2015. Qualitative and quantitative methods to determine miscibility in amorphous drug-polymer systems. *Eur J Pharm Sci* 77:106-111.
16. Bhattacharya S, Suryanarayanan R 2009. Local mobility in amorphous pharmaceuticals--characterization and implications on stability. *J Pharm Sci* 98(9):2935-2953.
17. Bhugra C, Pikal MJ 2008. Role of thermodynamic, molecular, and kinetic factors in crystallization from the amorphous state. *J Pharm Sci* 97:1329-1349.
18. Mehta M, Kothari K, Ragoonanan V, Suryanarayanan R 2016. Effect of water on molecular mobility and physical stability of amorphous pharmaceuticals. *Mol Pharmaceut* 13:1339-1346.
19. Zografi G, Newman A 2017. Interrelationships between structure and the properties of amorphous solids of pharmaceutical interest. *J Pharm Sci* 106:5-27.

20. Dill KA, Bromberg S. 2011. *Molecular Driving Forces: Statistical Thermodynamics in Chemistry, Physics, Biology, and Nanoscience*. New York: Garland Science. p 756.
21. Hildebrand JH, Scott RL. 1962. *Regular Solutions*. Englewood Cliffs, NJ: Prentice-Hall.
22. Flory PJ. 1953. *Principles of Polymer Chemistry*. Ithaca, New York: Cornell University Press.
23. Rubinstein M, Colby RH. 2003. *Polymer Physics*. New York: Oxford University Press.
24. Barton AFM. 1983. *Handbook of Solubility Parameters and Other Cohesion Parameters*. Boca Raton, FL: CRC Press.
25. Hancock BC, York P, Rowe RC 1997. The use of solubility parameters in pharmaceutical dosage form design. *Int J Pharm* 148:1-21.
26. Zhao Y, Inbar P, Chokshi HP, Malick AW, Choi DS 2011. Prediction of the thermal phase diagram of amorphous solid dispersions by Flory-Huggins theory. *J PharmSci* 100:3196-3207.
27. Tian Y, Booth J, Meehan E, Jones DS, Li S, Andrews GP 2013. Construction of drug-polymer thermodynamic phase diagrams using Flory-Huggins interaction theory: identifying the relevance of temperature and drug weight fraction to phase separation within solid dispersions. *Molecular pharmaceutics* 10(1):236-248.
28. Olabis O, Robeson LM, Shaw MT. 1979. *Polymer-Polymer Miscibility*. New York: Academic Press.
29. Marsac PJ, Shamblin SL, Taylor LS 2006. Theoretical and practical approaches for prediction of drug-polymer miscibility and solubility. *Pharm Res* 23:2417-2426.
30. Marsac PJ, Konno H, Taylor LS 2006. A comparison of the physical stability of amorphous felodipine and nifedipine systems. *Pharm Res* 23(10):2306-2316.
31. Xiang T-X, Anderson BD 2013. Molecular dynamics simulation of amorphous indomethacin-poly(vinylpyrrolidone) glasses: solubility and hydrogen bonding interactions. *J Pharm Sci* 102:876-891.
32. Xiang T-X, Anderson BD 2017. Molecular dynamics simulation of amorphous hydroxypropylmethylcellulose and its mixtures with felodipine and water. *J Pharm Sci* 106:803-816.
33. Hansen CM. 1967. *The three dimensional solubility parameter and solvent diffusion coefficient*. ed., Copenhagen: Technical University of Denmark.
34. Hansen CM 1969. Universality of the solubility parameter. *Industrial & Engineering Chemistry Product Research and Development* 8(1):2-11.
35. Karger BL, Snyder LR, Eon C 1976. An expanded solubility parameter treatment for classification and use of chromatographic solvents and adsorbents. *J Chromatogr, A* 125:71-88.
36. Thakral S, Thakral NK 2013. Prediction of drug-polymer miscibility through the use of solubility parameter based Flory-Huggins interaction parameter and the experimental validation. *J Pharm Sci* 102:2254-2263.
37. Hoi Y, Yamaura K, Matsuzawa S 1992. A lattice treatment of crystalline solvent-amorphous polymer mixtures on melting point depression. *J Phys Chem* 96:10584-10586.
38. Marsac PJ, Li T, Taylor LS 2009. Estimation of drug-polymer miscibility and solubility in amorphous solid dispersions using experimentally determined interaction parameters. *Pharm Res* 26:139-150.
39. Knopp MM, Tajber L, Tian Y, Olesen NE, Jones DS, Kozyra A, Lobmann K, Paluch K, Brennan CM, Holm R, Healy AM, Andrews GP, Rades T 2015. Comparative study of different methods for the prediction of drug-polymer solubility. *Mol Pharmaceut* 12:3408-3419.
40. Paudel A, Van Humbeeck J, Van den Mooter G 2010. Theoretical and experimental investigation on the solid solubility and miscibility of naproxen in poly(vinylpyrrolidone). *Mol Pharm* 7:1133-1148.
41. Rask MB, Knopp MM, Olesen NE, Holm R, Rades T 2016. Influence of PVP/VA copolymer composition on drug-polymer solubility. *Eur J Pharm Sci* 85:10-17.
42. Neau SH, Bhandakar SV, Hellmuth EW 1997. Differential molar heat capacities to test ideal solubility estimations. *Pharm Res* 14:601-605.

43. Lehmkemper K, Kyeremateng SO, Heinzerling O, Degenhardt M, Sadowski G 2017. Long-term physical stability of PVP- and PVPVA-amorphous solid dispersions. *Mol Pharm* 14:157-171.
44. Luebbert C, Huxoll F, Sadowski G 2017. Amorphous-amorphous phase separation in API/polymer formulations. *Molecules* 22:296.
45. Lin D, Huang Y 2010. A thermal analysis method to predict the complete phase diagram of drug-polymer solid dispersions. *Int J Pharm* 399:109-115.
46. Knopp MM, Olesen NE, Huang Y, Holm R, Rades T 2015. Statistical analysis of a method to predict drug-polymer miscibility. *J Pharm Sci* 105:362-367.
47. Manias E, Utracki LA. 2014. Thermodynamics of Polymer Blends. In Utracki LA, Wilkie C, editors. *Polymer Blends Handbook*, Dordrecht: Springer Science + Business Media. p 171-289.
48. Baghel S, Cathcart H, O'Reilly NJ 2016. Theoretical and experimental investigation of drug-polymer interaction and miscibility and its impact on drug supersaturation in aqueous medium. *Eur J Pharm Sci Biopharm* 107:16-31.
49. Koningsveld R, Stockmayer W, Nies E. 2001. *PolymerPhase Diagram: A Text Book*. Oxford: Oxford University Press.
50. Xiang T-X, Anderson BD 2013. Molecular dynamics simulation of amorphous indomethacin. *Mol Pharmaceut* 10:102-114.
51. Xiang T-X, Anderson BD 2004. A molecular dynamics simulation of reactant mobility in an amorphous formulation of a peptide in poly(vinylpyrrolidone). *J Pharm Sci* 93:855-876.
52. Xiang T-X, Anderson BD 2005. Distribution and effect of water content on molecular mobility in poly(vinylpyrrolidone) glasses: A molecular dynamics simulation. *Pharm Res* 22:1205-1214.
53. Xiang T-X, Anderson BD 2014. Water uptake, distribution, and mobility in amorphous poly(D,L-lactide) by molecular dynamics simulation. *J Pharm Sci* 103:2759-2771.
54. Hancock BC, Shamblin SL, Zografi G 1995. Molecular mobility of amorphous pharmaceutical solids below their glass transition temperatures. *Pharm Res* 12:799-806.
55. Matsumoto T, Zografi G 1999. Physical properties of solid molecular dispersions of indomethacin with poly(vinylpyrrolidone) and poly(vinylpyrrolidone-co-vinyl-acetate) in relation to indomethacin crystallization. *Pharm Res* 16(11):1722-1728.
56. Alonzo DE, Gao Y, Zhou D, Mo H, Zhang GG, Taylor LS 2011. Dissolution and precipitation behavior of amorphous solid dispersions *J Pharm Sci* 100:3316-3331.
57. Rumondor ACF, Konno H, Marsac PJ, Taylor LS 2010. Analysis of the moisture sorption behavior of amorphous drug-polymer blends. *J Appl Polym Sci* 117:1055-1603.
58. Taylor LS, Zografi G 1997. Spectroscopic characterization of interactions between PVP and indomethacin in amorphous molecular dispersions. *Pharm Res* 14:1691-1698.
59. Sun Y, Tao J, Zhang GG, Yu L 2010. Solubilities of crystalline drugs in polymers: an improved analytical method and comparison of solubilities of indomethacin and nifedipine in PVP, PVP/VA, and PVAc. *J Pharm Sci* 99:4023-4031.
60. Tao J, Sun Y, Zhang GG, Yu L 2009. Solubility of small-molecule crystals in polymers: D-mannitol in PVP, indomethacin in PVP/VA, and nifedipine in PVP/VA. *Pharm Res* 26:855-864.
61. Rumondor AC, Marsac PJ, Stanford LA, Taylor LS 2009. Phase behavior of poly(vinylpyrrolidone) containing amorphous solid dispersions in the presence of moisture. *Mol Pharmaceut* 6:1492-1505.
62. Rumondor AC, Taylor LS 2010. Effect of polymer hygroscopicity on the phase behavior of amorphous solid dispersions in the presence of moisture. *Mol Pharmaceut* 7(2):477-490.
63. Lu Q, Zografi G 1998. Phase behavior of binary and ternary amorphous mixtures containing indomethacin, citric acid, and PVP. *Pharm Res* 15:1202-1206.
64. Newman A, Engers D, Bates S, Ivanisevic I, Kelly RC, Zografi G 2008. Characterization of amorphous API:Polymer mixtures using X-ray powder diffraction *J Pharm Sci* 97:4840-4856.



65. Reddy R, Chang LL, Luthra S, Collins G, Lopez C, Shamblin SL, Pikal MJ, Gatlin LA, Shalaev EY 2009. The glass transition and sub-T(g)-relaxation in pharmaceutical powders and dried proteins by thermally stimulated current. *J Pharm Sci* 98(1):81-93.
66. Yoshioka M, Hancock BC, Zografi G 1995. Inhibition of indomethacin crystallization in poly(vinylpyrrolidone) coprecipitates. *J Pharm Sci* 84:983-986.
67. Yuan X, Xiang T-X, Anderson BD, Munson EJ 2015. Hydrogen bonding interactions in amorphous indomethacin and its amorphous solid dispersions with poly(vinylpyrrolidone) and poly(vinylpyrrolidone-co-vinyl acetate) studied using <sup>13</sup>C solid-state NMR. *Mol Pharmaceut* 12:4518-4528.
68. Anderson BD, Rytting JH, Lindenbaum S, Higuchi T 1975. A calorimetric study of the self-association of primary alcohols in isooctane. *J Phys Chem* 79:2340-2344.
69. Anderson BD, Rytting JH, Higuchi T 1978. Vapor pressure studies of the self-association of alcohols in isooctane. I. The effect of chain length. *Int J Pharm* 1:15-31.
70. Rytting JH, Anderson BD, Higuchi T 1978. Vapor pressure studies of the self-association of alcohols in isooctane. 2. The effect of chain branching. *J Phys Chem* 82:2240-2246.
71. Kubinyi H. 1993. QSAR: Hansch analysis and related approaches. Weinheim, Germany: VCH.
72. Yalkowsky SH, Roseman TJ. 1981. Solubilization of drugs by cosolvents. In Yalkowsky SH, editor *Techniques of Solubilization of Drugs*, New York: Marcel Dekker. p 91-134.
73. Yalkowsky SH, Valvani SC 1980. Solubility and partitioning I: solubility of nonelectrolytes in water. *J Pharm Sci* 69:912-922.
74. MacCallum JL, Tieleman DP 2002. Structures of neat and hydrated 1-octanol from computer simulations. *J Am Chem Soc* 124:15085-15093.
75. Fouad WA, Wang L, Haghmoradi A, Gupta SK, Chapman WG 2015. Understanding the thermodynamics of hydrogen bonding in alcohol-containing mixtures: Self association. *J Phys Chem B* 119:14086-14101.
76. Gracia M, Sanchez F, Perez P, Valero J, Losa CG 1992. Vapour pressures of (butan-1-ol + hexane) at temperatures between 283.10 K and 323.12 K. *J Chem Thermodynamics* 24:463-471.
77. Van Ness HC, Soczek CA, Kochar NK 1967. Thermodynamic excess properties for ethanol-n-heptane. *J Chem Eng Data* 12:346-351.
78. Flory PJ 1944. Thermodynamics of heterogeneous polymers and their solutions. *J Chem Phys* 12:425-438.
79. Kretschmer CB, Wiebe R 1954. Thermodynamics of alcohol-hydrocarbon mixtures. *J Chem Phys* 22:1697-1701.
80. Acree WE. 1984. *Thermodynamic Properties of Nonelectrolyte Solutions*. New York: Academic Press.
81. Painter PC, Park Y, Coleman MM 1988. Hydrogen bonding in polymer blends. 2. Theory. *Macromolecules* 21:66-72.
82. Painter PC, Park Y, Coleman MM 1989. Thermodynamics of hydrogen bonding in polymer blends. 1. Application of association models. *Macromolecules* 22:570-579.
83. Painter PC, Graf J, Coleman MM 1990. A lattice model describing hydrogen bonding in polymer mixtures. *J Chem Phys* 92:6166-6174.
84. Coleman MM, Graf JF, Painter PC. 1991. *Specific Interactions and the Miscibility of Polymer Blends*. Lancaster, PA: Technomic Publishing.
85. Coleman MM, Painter PC. 2006. *Miscible Polymer Blends: Background and Guide for Calculations and Design*. Lancaster, PA: Technomic Publishing.
86. Park Y, Veytsman B, Coleman MM, Painter PC 2005. The miscibility of hydrogen-bonded polymer blends: Two self-associating polymers. *Macromolecules* 38:3703-3707.

87. Park Y, Graf J, Painter PC 2007. An association model describing the mixing of two self-associating fluids. *Fluid Phase Equilibria* 254:101-111.
88. De Vito F, Veytsman B, Painter PC, Kokini JL 2015. Simulation of the effect of hydrogen bonds on water activity of glucose and dextran using the Veytsman model. *Carbohydrate polymers* 117:236-246.
89. Painter PC, Veytsman B, Kumar S, Shenoy S, Graf JF, Xu Y, Coleman MM 1997. Intramolecular screening effects in polymer mixtures. 1. Hydrogen-bonded polymer blends. *Macromolecules* 30:932-942.
90. Hu Y, Painter PC, Coleman MM 2000. On the infrared spectroscopic determination of self- and interassociation equilibrium constants used in the prediction of the phase behavior of hydrogen bonded polymer blends. *Macromolecular Chemistry and Physics* 201:470-477.
91. Kuo S-W, Shih C-C, Shieh J-S, Chang F-C 2004. Specific interactions in miscible polymer blends of poly(2-hydroxypropyl methacrylate) with polyvinylpyrrolidone. *Polym Int* 53:218-224.
92. Painter PC, Coleman MM. 2000. Hydrogen bonding systems. In Paul DR, Bucknall CB, editors. *Polymer Blends*, New York: Wiley.
93. Gross J, Sadowski G 2000. Application of perturbation theory to a hard-chain reference fluid: an equation of state for square-well chains. *Fluid Phase Equilibria* 168:183-199.
94. Gross J, Sadowski G 2001. Perturbed-chain SAFT: An equation of state based on perturbation theory for chain molecules. *Ind Eng Chem Res* 40:1244-1260.
95. Prudic A, Ji Y, Sadowski G 2014. Thermodynamic phase behavior of API/polymer solid dispersions. *Mol Pharmaceut* 11:2294-2304.
96. Chapman WG, Jackson G, Gubbins KE 1988. Phase equilibria of associating fluids: Chain molecules with multiple bonding sites. *Mol Phys* 65:1057-1079.
97. Prudic A, Lesniak A-K, Ji Y, Sadowski G 2015. Thermodynamic phase behaviour of indomethacin/PLGA formulations. *Eur J Pharm Sci Biopharm* 93:88-94.
98. Prudic A, Kleetz T, Korf M, Ji Y, Sadowski G 2014. Influence of copolymer composition on the phase behavior of solid dispersions. *Mol Pharmaceutics* 11:4189-4198.
99. Prudic A, Ji Y, Luebbert C, Sadowski G 2015. Influence of humidity on the phase behavior of API/polymer formulations. *Eur J Pharm Biopharm* 94:352-362.
100. Kyeremateng SO, Pudlas M, Woehrle GH 2014. A fast and reliable empirical approach for estimating solubility of crystalline drugs in polymers for hot melt extrusion formulations. *J Pharm Sci* 103:2847-2858.

Figure Legends.

Figure 1. Number of articles found in a mid-2017 SciFinder© literature search for the keyword “amorphous” and “pharmaceutical” versus the year of publication.

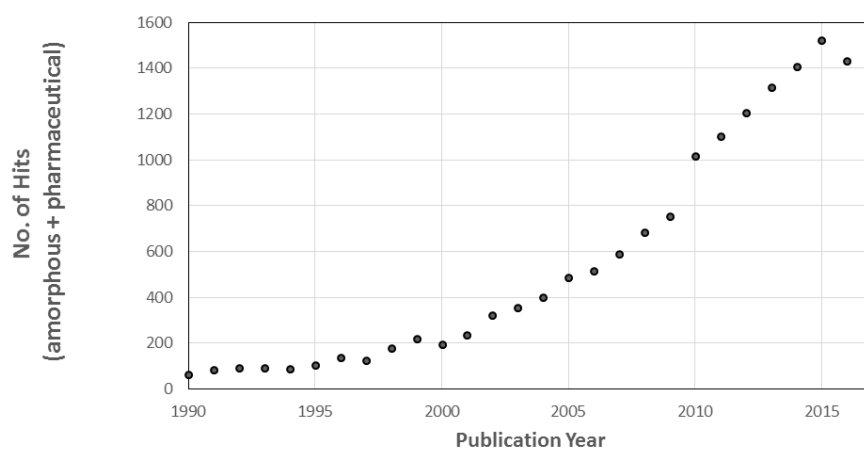
Figure 2. Free energy of mixing profiles versus mole fraction of butanol generated from a report by Gracia et al.<sup>76</sup> on the vapor pressures above solutions of 1-butanol and n-hexane at 10 °C (---), 25 °C (— — —), and 50 °C (——). *Lower:* The calculated ideal free energies of mixing divided by RT,  $\Delta G_{\text{ideal}}/RT$ , assuming the ideal entropy contribution from random mixing and zero enthalpy of mixing. *Middle:* Observed free energies of mixing over RT,  $\Delta G_{\text{mix}}/RT$ , from the experimental vapor pressure data of Gracia et al. *Upper:* Excess free energies of mixing over RT,  $\Delta G_{\text{excess}}/RT$  obtained from the difference between the experimental and ideal free energies at each solution composition and temperature.

Figure 3. Calculated values of  $\chi_{AB}$  according to Eq. 6 obtained from the data in Fig. 2 at the three temperatures (10 °C (---), 25 °C (— — —), and 50 °C (——) versus the mole fraction of butanol.

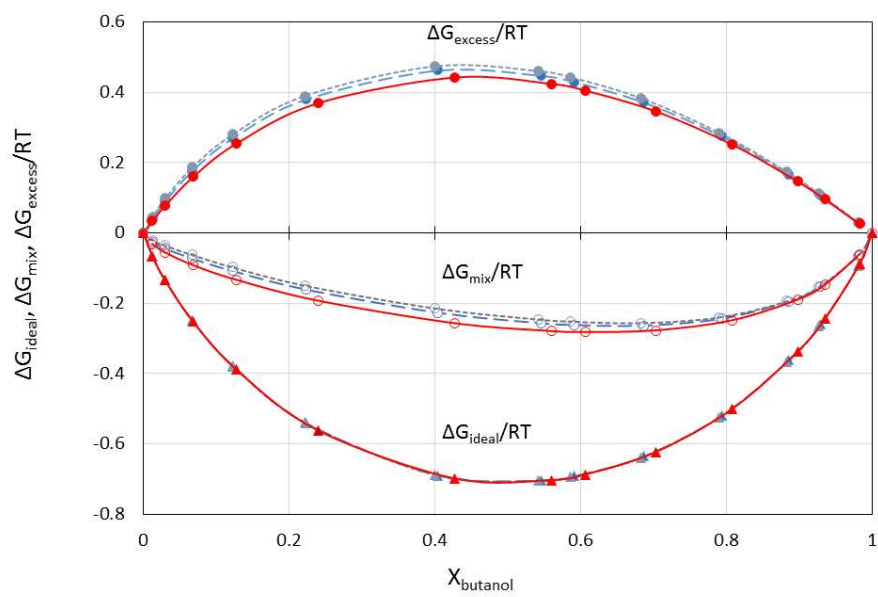
Figure 4. Profiles for  $\Delta H_{\text{mix}}/RT$  (upper),  $\Delta G_{\text{mix}}/RT$  (middle), and  $-\Delta S_{\text{mix}}/R$  (lower) versus the mole fraction of ethanol at 5 °C (---), 25 °C (— — —), and 40 °C (——) calculated from vapor-liquid equilibria and calorimetry data<sup>77</sup> for mixing ethanol and heptane.  $\Delta G_{\text{mix}}/RT$  is slightly negative indicating that ethanol and heptane are completely miscible at these temperatures. A substantial enthalpy-entropy compensation is evident as decreases in the positive enthalpy of mixing at lower temperature are counterbalanced by less favorable excess entropies of mixing, leading to nearly superimposable profiles for the free energies of mixing,  $\Delta G_{\text{mix}}/RT$ , over this temperature range.

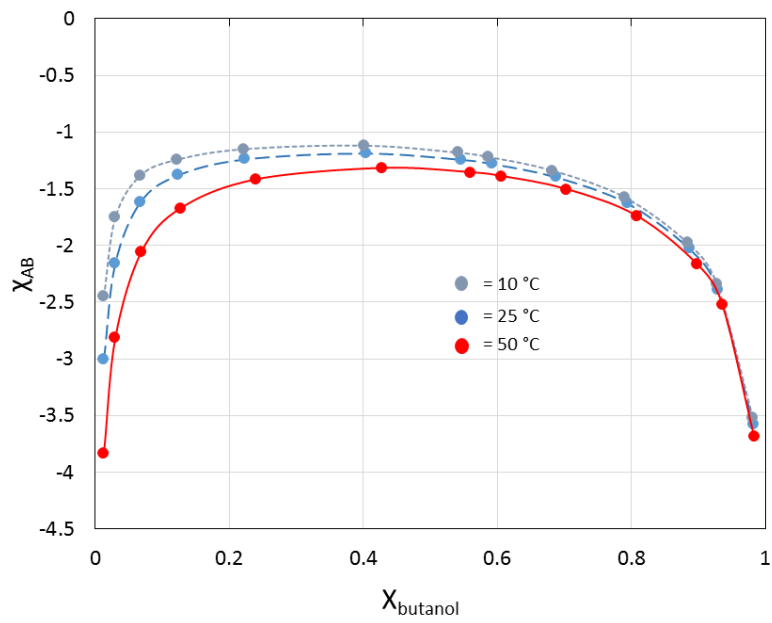
Figure 5. Calculated values of  $\chi_{AB}$  obtained from the data in Fig. 4 at three temperatures (10 °C (---), 25 °C (— — —), and 50 °C (——)) versus the mole fraction of butanol. Upper curves:  $\chi_{AB}$  values calculated directly from enthalpies of mixing according to Eq. 4. Lower curves:  $\chi_{AB}$  values calculated from Eq. 6.

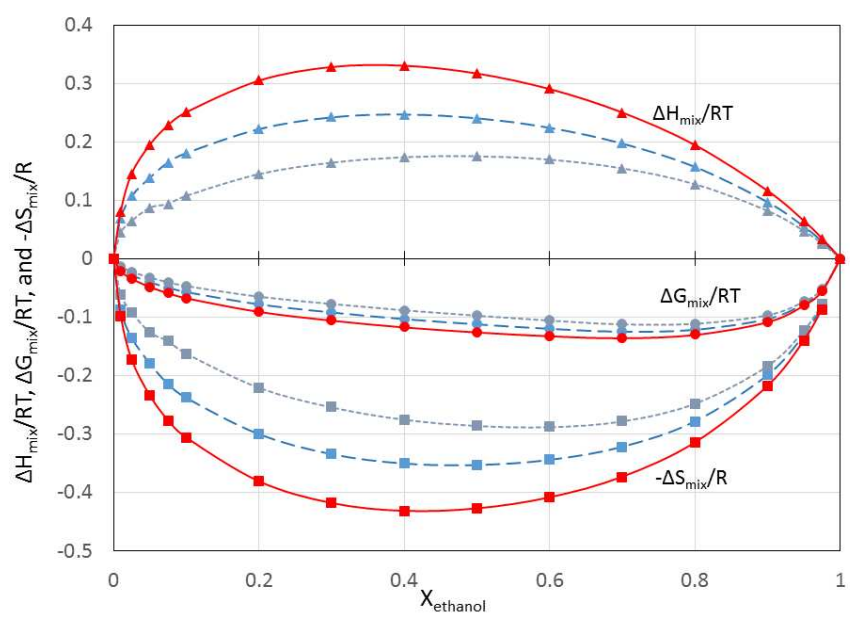
Figure 6. Chemical structure of indomethacin and its depiction as a chain consisting of five spherical segments (light grey) and six association sites,  $N_i^{\text{association}}$ , within PC-SAFT.<sup>95</sup> Reprinted with permission from Prudic et al.<sup>95</sup> Copyright 2014 American Chemical Society.

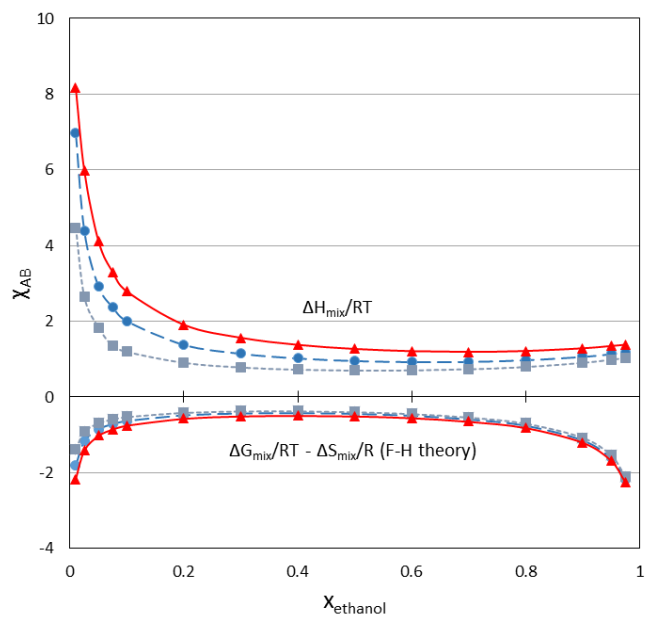


ACCEPTED MANUSCRIPT

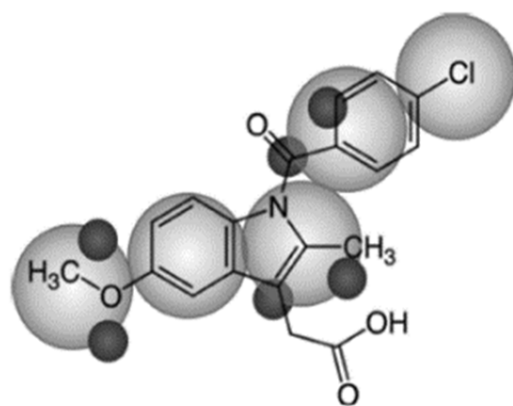












ACCEPTED MANUSCRIPT